An Ultra-compact Colorless 50:50 Coupler Based on PhC-like Metamaterial Structure

Luluzi Lu, Minming Zhang*, Feiya Zhou, and Deming Liu
School of Optical and Electrical Information, Huazhong University of Science and Technology, Wuhan, 430074, China
**mmz@mail.hust.edu.cn*

Abstract: A novel PhC-like metamaterial structure with low fabricating accuracy requirements is proposed. We design and fabricate a 2.6μm×2.6μm coupler employing such structure. The measured excess loss of each port is less than 1dB over 60nm.
OCIS codes: (160.3918) Metamaterials; (130.3120) Integrated optics devices; (130.5296) Photonic crystal waveguides

1. Introduction

Metamaterial structures have drawn more and more attentions recently since silicon photonics and corresponding fabrication technology have experienced a remarkable progress. The geometrical structure variations at subwavelength (SW) dimension can provide a large scale of effective index engineering as long as those variations are small enough to suppress diffraction [1]. There have been many reported functional components based on SW structure, such as directional coupler (DC), optical cross [1,2], wavelength router [2,3], polarization beam splitter [4] etc. Among those, the team of Jelena Vuckovic et al. [3] and the team of Rajesh Menon et al. [4] provided two novel inverse methods to design objective components. The former may cost much computing time and the latter comes with substantial time reduction. However it's obviously that both of them require high etching accuracy and some details get lost inevitably due to a large number of sharp corners or complicated acute angles. In this paper, we provide an alternative solution to the mentioned problem.

A novel photonic-crystal-like (PhC-like) metamaterial structure is proposed to drastically reduce the fabricating accuracy requirements as shown in Fig.1 (a). The circle voids can avoid the sharp angles and be much more easier in fabrication since the fabrication of slab PhC components is quite developed. By optimizing the circle combination and radius, one can use one-step etching to fabricate the device to improve the manufacture efficiency greatly. The simulated insertion loss (IL) of each port is less than 3.6dB over 100nm using an improved inverse design method. The measured IL is less than 4dB with the excess loss of each port less than 1dB over the observable 60nm bandwidth and shows good agreements with simulation results.

2. Operation principle and simulation results

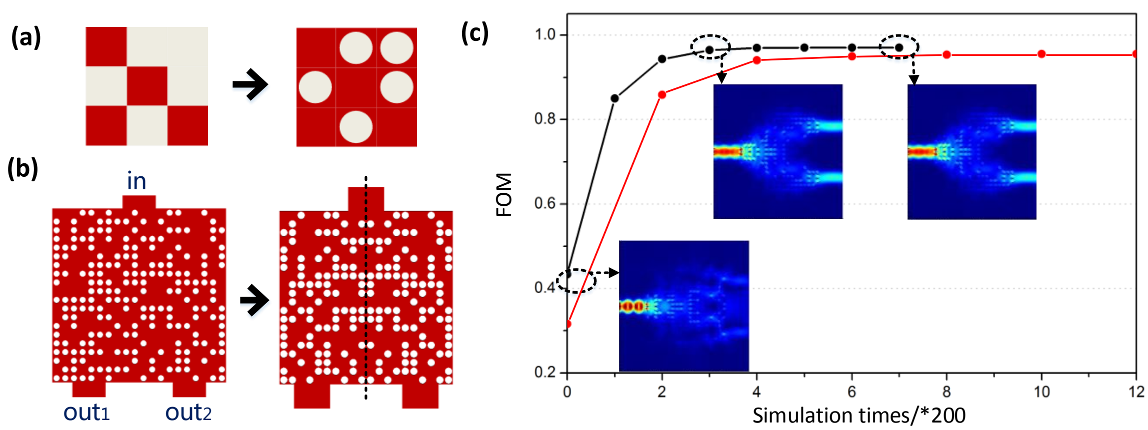

Fig.1 (a) the top view of etching void change, (b) the top view of the random pixel combination (left) and the axisymmetric initial pixel combination (right), (c) the convergence process of the FOM for the random (red) and the axisymmetric (black) initial pixel combinations, the insertions are the simulated optical distribution after 0, 3, 7 iterations respectively for the axisymmetric initial pixel combination, one iteration contains 200 times of simulation.

To begin with, a 2.6μm×2.6μm region is discretized into 20×20 pixels with the size of 130nm×130nm in consideration of process conditions. A random 20×10 binary matrix is set to be the initial of our design: 1 stands for no etching and 0 stands for a circle void of radius r etched into silicon respectively. Each element of the 20×10 binary matrix corresponds to two axisymmetric pixels along the middle axis as shown in Fig.1 (b). The axisymmetric character of pixel combination is kept during the following optimization process so that the imbalance of outputs is negligible and it also comes with a half reduction in iteration time above all (Fig.1 (c)). The figure of merit (FOM) for optimization is defined as $\mathrm{FOM} = 1 - (1-\alpha)\cdot(|t_1 - 0.5| + |t_2 - 0.5|) - \alpha \cdot |t_1 - t_2|$, t1 and t2 stand for the transmissions of the output ports respectively, α is the weight of output imbalance and set to 0 here. The radius r is set to 45nm at first. The waveguide width is set to 500nm and the separation of output ports is set to 1μm.

Then the direct-binary-search (DBS) optimization algorithm is used to figure out the optimal overall void combination as the optimization problem may have a number of possible pixel combinations [4]. We toggle the state of the two axisymmetric pixels and evaluate the FOM. If the FOM get improved, then the new state is kept and the next two pixels are toggled. We use the 2D FDTD simulations for timesaving. The material dispersion is considered. One iteration ends when all the pixel states are disposed. When the FOM exhibits no improvement after one iteration, the optimization ends. We can see that the optimization algorithm converges fast in Fig.1 (c) and the FOM (in black) tend to become stable after 3 times of iterations.

Since the DBS is quite sensitive to the initial value and tends to converge prematurely in local optima [5], the optimized results are usually not ideal with random initials. Particularly, the proposed device is a 50:50 coupler, so we can use an axisymmetric initial combination instead of a totally random one, this may help avoid that problem. The optimum combinations for an axisymmetric initial and a random initial are shown in Fig.2 (a) and (b) respectively. The corresponding IL can be seen in Fig.2 (c): the black line stands for the outputs for the axisymmetric initial, the red and blue lines stand for the two outputs for the random initial. The transmission imbalance for the random initial is nearly 0.3dB and the excess loss is higher than that of the axisymmetric one. The degradation of the optimum transmissions is caused by the item of imbalance weight in FOM, which can be omitted for the axisymmetric case.

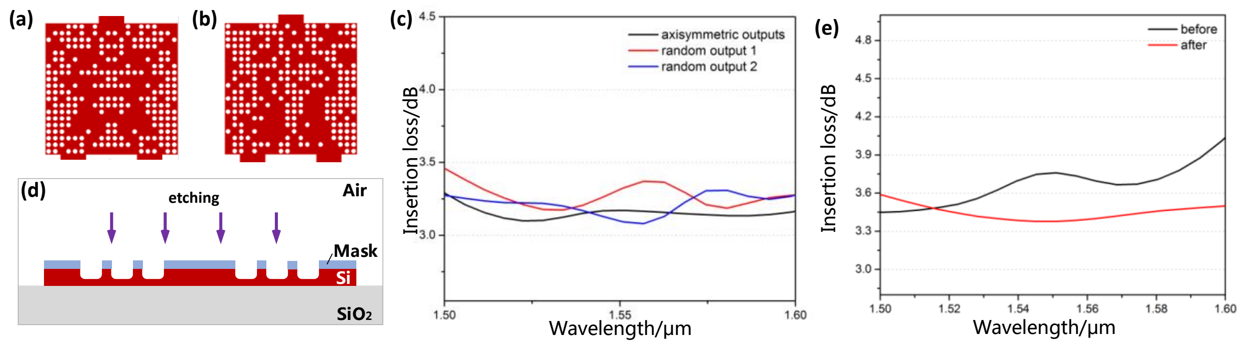

Fig.2 (a) and (b) are top views of the simulated optimum pixel combination with axisymmetric and random initials respectively, (c) the IL of (a) (black) and (b) (red, blue) by 2D simulations, (d) the cross section of etching depth, (e) the IL before (black) and after (red) radius optimization by 3D simulations.

The 3D FDTD simulations are used to make further optimization. Since the device is expected to be fabricated with one-step ICP etching on a 220nm-thick SOI, the etching depth of the voids is not the ideal 220nm in our case as shown in Fig.2 (d). The radius r of the circle voids is selected as an optimization parameter for different etching depth. The upper limit of 60nm and the lower limit of 40nm are imposed on the void radius. At last, a radius of 48nm is chosen in case of an empirical etching depth of 140nm. Fig.2 (e) shows the IL before (in black) and after (in red) the radius optimization.

3. Experiment results

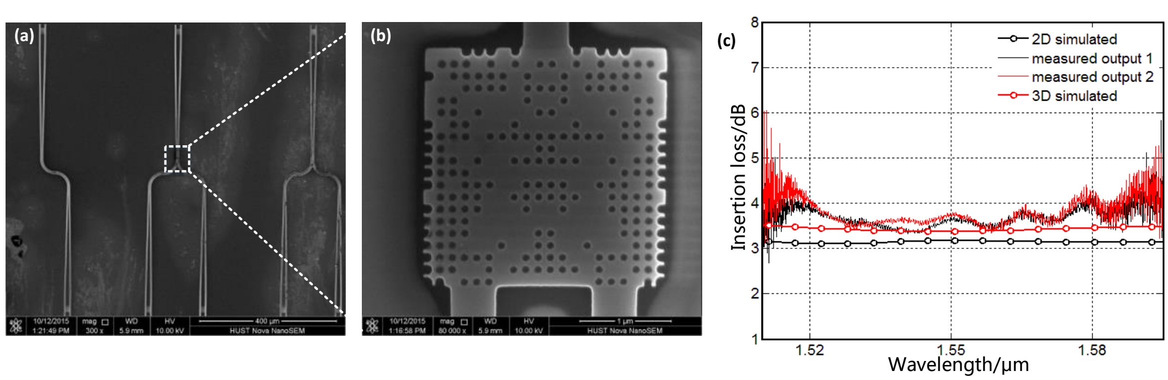

Fig.3 (a) and (b) are the scanning electron micrographs of the fabricated device, (c) the simulated and measured IL of the 50:50 coupler.

A scanning electron micrograph of the fabricated device is shown in Fig.3 (a). The details are shown in Fig.3 (b). The transmission spectrums of the two output ports are shown in Fig.3 (c). The normalized IL for each output port is defined as $\mathrm{IL} = -10\lg(\mathrm{t}/\mathrm{T})$, t and T correspond to the measured transmittances of each output ports of the device and the reference waveguide with only two coupling gratings respectively. We can see from Fig.3 (c) that the IL of each output port is less than 4dB over 60nm bandwidth and exhibits good uniformity. In fact, the device is designed to be colorless over 100nm bandwidth, but we can just observe the transmissions in about 60nm bandwidth due to the limit bandwidth of the vertical coupling grating. Those regular jitter at longer wavelengths may be caused by the imperfect edge of the coupling region. Above all, the device shows good tolerance with fabrication deviation.

4. Conclusions

We propose and experimentally demonstrate a colorless 50:50 coupler assisted by a novel PhC-like subwavelength structure. The footprints of the coupler is 2.6μm×2.6μm. The measured results show that the IL of our device is less than 4dB with the excess loss of each port less than 1dB over 60nm bandwidth. The proposed device could be a potential and promising component for future all optical wavelength division multiplexing (WDM) networks. The design method can adapt to extensive linear optical components.

5. Acknowledgment

This work is partially supported by the National High Technology Research and Development Program of China (863 Program, Grand No. 2015AA015504) and the Major Project of Science and Technology Innovation Program of Hubei Province of China (Grand No. 2014AAA006) and National Natural Science Foundation of China (Grand No. 61107051) .

6. References

[1] Bock P J, Cheben P, Schmid J H, “Subwavelength grating periodic structures in silicon-on-insulator: a new type of microphotonic waveguide,” Opt. Express 18, 20251-20262 (2010).

[2]. Schmid J H, Cheben P, Bock P J, “Refractive index engineering with subwavelength gratings in silicon microphotonic waveguides,” Photonics Journal, IEEE 3, 597-607 (2011).

[3] Piggott A Y, Lu J, Lagoudakis K G, “Inverse design and demonstration of a compact and broadband on-chip wavelength demultiplexer,” Nature Photonics 9, 374-377 (2015).

[4] Shen B, Wang P, Polson R, “An integrated-nanophotonics polarization beamsplitter with 2.4× 2.4 μm2 footprint,” Nature Photonics 9, 378-382 (2015).

[5] Kim G, Dominguez-Caballero J A, Lee H, “Increased photovoltaic power output via diffractive spectrum separation,” Physical review letters, 110, 123901 (2013).